Using Polynomial Loss and Uncertainty Information for Robust Left Atrial and Scar Quantification and Segmentation

Tewodros Weldebirhan Arega, Stéphanie Bricq, Fabrice Meriaudeau

Using Polynomial Loss and Uncertainty Information for Robust Left Atrial and Scar Quantification and Segmentation

Tewodros Weldebirhan Arega(✉), Stéphanie Bricq, and Fabrice Meriaudeau

ImViA Laboratory, Université Bourgogne Franche-Comté, Dijon, France
✉tewdrosw[at]gmail.com

Abstract. Automatic and accurate segmentation of the left atrial (LA) cavity and scar can be helpful for the diagnosis and prognosis of patients with atrial fibrillation. However, automating the segmentation can be difficult due to the poor image quality, variable LA shapes, and small discrete regions of LA scars. In this paper, we proposed a fully-automatic method to segment LA cavity and scar from Late Gadolinium Enhancement (LGE) MRIs. For the loss functions, we propose two different losses for each task. To enhance the segmentation of LA cavity from the multi-center dataset, we present a hybrid loss that leverages Dice loss with a polynomial version of cross-entropy loss (PolyCE). We also utilize different data augmentations that include histogram matching to increase the variety of the dataset. For the more difficult LA scar segmentation, we propose a loss function that uses uncertainty information to improve the uncertain and inaccurate scar segmentation results. We evaluate the proposed method on the Left Atrial and Scar Quantification and Segmentation (LAScarQS 2022) Challenge dataset. It achieves a Dice score of 0.8897 and a Hausdorff distance (HD) of 16.91mm for LA cavity and a Dice score of 0.6406 and sensitivity of 0.5853 for LA scar. From the results, we notice that for LA scar segmentation, which has small and irregular shapes, the proposed loss that utilizes the uncertainty estimates generated by the scar yields the best result compared to the other loss functions. For the multi-center LA cavity segmentation, we observe that combining the region-based Dice loss with the pixelwise PolyCE can achieve a good result by enhancing the segmentation result in terms of both Dice score and HD. Furthermore, using moderate-level data augmentation with histogram matching improves the model's generalization capability. Our proposed method won the Left Atrial and Scar Quantification and Segmentation (LAScarQS 2022) Challenge.

Keywords: Cardiac MRI · Late Gadolinium Enhancement MRI · Left Atrium · Scar quantification · Segmentation · Deep learning · PolyLoss · Uncertainty

1 Introduction

Atrial fibrillation (AF) is an irregular and often very rapid heart rhythm (arrhythmia). During atrial fibrillation, the heart's upper chambers (the atria) beat

irregularly and out of synchronization with the heart's lower chambers (the ventricles). AF increases the risk of stroke, heart failure, and other heart-related complications [6]. One of the most commonly used techniques to treat AF patients is radio-frequency catheter ablation using the pulmonary vein (PV) isolation [27].

Late Gadolinium Enhancement (LGE), sometimes called delayed-enhancement MRI, is a gold standard imaging technique to visualize and quantify the left atrial (LA) scars. In a clinical routine, human experts generally segment the LA anatomy and LA scars manually. Manual segmentation is time-consuming and suffers from intra- and inter-observer variability. This problem can be addressed by automating the segmentation. However, automatic segmentation of LA anatomy and LA scars from LGE MRI is still challenging due to poor image quality, variable LA shapes, thin LA walls, and small isolated regions of the LA scars [16].

Few studies have been proposed to segment LA cavity from LGE MR images. Gao *et al.* (2010) [7] and Zhu *et al.* (2013) [32] utilized region-based active-contour and variational region growing with shape prior respectively to segment LA cavity. Tao *et al.* (2016) [25] used atlas-based methods leveraging auxiliary images with better anatomical information to help the LA cavity segmentation from LGE MRI [17]. However, accurately segmenting LA cavity using these conventional methods depend on additional information such as shape prior or auxiliary images [17]. Recently, deep learning-based algorithms have been successfully applied to segment LA cavity from LGE MRI. Vesal *et al.* (2018) [26] proposed a 3D U-Net with dilated convolutions at the bottleneck of the network and residual connections between the encoder blocks to incorporate local and global information. Chen *et al.* (2018) [5] adopted multi-task learning to perform both LA cavity segmentation and pre/post ablation classification. Other works [10, 28, 30] utilized a two-stage cascaded segmentation framework to first locate the region of interest (ROI) that covers the atrial cavity, then used a second network to segment LA cavity from the cropped ROI. The main problem with these cascaded approaches is that they can be time- and resource-intensive.

Recently, semi-automatic and fully-automatic deep learning based methods have been widely used to segment scar [1, 21, 31]. For LA scar segmentation, some studies proposed to use non-deep learning based methods such as thresholding [22, 24], clustering [23], deformable and graph-based methods [11, 12]. Although these conventional methods have shown encouraging results, they rely on initial manual segmentation of the LA cavity. Deep learning methods have been presented to automatically segment LA scar from LGE MRIs. Li et al. [14] proposed to use graph-cuts with multi-scale CNNs to automatically segment LA scar. Other works utilized multi-task learning to jointly segment LA cavity and scar [16, 29].

In this paper, we proposed a fully automatic deep learning based method that leverages a polynomial loss and an uncertainty based loss to segment LA cavity from multi-center LGE MRIs and LA scar from single-center LGE MRIs, respectively. To increase the variety of the dataset, we also employ various

data augmentation techniques, including histogram matching. We evaluated our method on Left Atrial and Scar Quantification and Segmentation (LAScarQS 2022) Challenge dataset. The proposed losses achieve the best result compared to other losses in both the multi-center LA cavity segmentation and the highly imbalanced LA scar segmentation. In addition, the employed data augmentation techniques improve the model's generalization on the LA cavity segmentation from multi-center images.

2 Dataset

The Left Atrial and Scar Quantification and Segmentation Challenge (LAScarQS 2022) [1] consists of 200 LGE MRIs acquired in a real clinical environment from patients suffering Atrial fibrillation (AF). All the LGE MRIs were collected from three different clinical centers. The images from the first center (University of Utah) were acquired using Siemens Avanto 1.5T or Vario 3T. The voxel resolution of the images was $1.25 \times 1.25 \times 2.5$ mm. The LGE MRIs from the second center (Beth Israel Deaconess Medical Center) were acquired with Philips Achieva 1.5T. The spatial resolution of the images was $1.4 \times 1.4 \times 1.4$ mm. Similar to the second center, the images from the third center (King's College London) were acquired with a Philips Achieva 1.5T. The spatial resolution of the LGE MRI scan was $1.3 \times 1.3 \times 4.0$ mm. The challenge has two tasks. The first one focuses on left atrial blood pool segmentation from multi-center LGE MRIs. The second task focuses on segmentation of left atrial scar [15–17]. We declare that the segmentation method implemented for participation in the LAScarQS 2022 challenge has not used any pre-trained models nor extra MRI datasets other than those given by the organizers.

3 Methods

3.1 Network Architecture

For both LA cavity and LA scar segmentation, we employed a 3D segmentation network. The network architecture is based on 3D nnU-Net framework [9]. As demonstrated in Fig. 1, we altered the standard nnU-Net network architecture by adding Dropout at the network's middle layers [3] to lessen overfitting and improve generalization. The U-Net's encoder and decoder consist of 10 convolutional layers where each convolution is followed by instance normalization and Leaky ReLU (negative slope of 0.01) activation function. The kernel size of the convolution is $3 \times 3 \times 3$. During pre-processing, we resampled all the volumes to $0.625mm \times 0.625mm \times 1.0mm$ and $0.625mm \times 0.625mm \times 2.5mm$ for LA cavity segmentation and LA scar segmentation respectively (the median voxel spacing of the training cases). The intensity of every volume was normalized to have zero-mean and unit-variance.

[1] `https://zmic.fudan.edu.cn/lascarqs22`

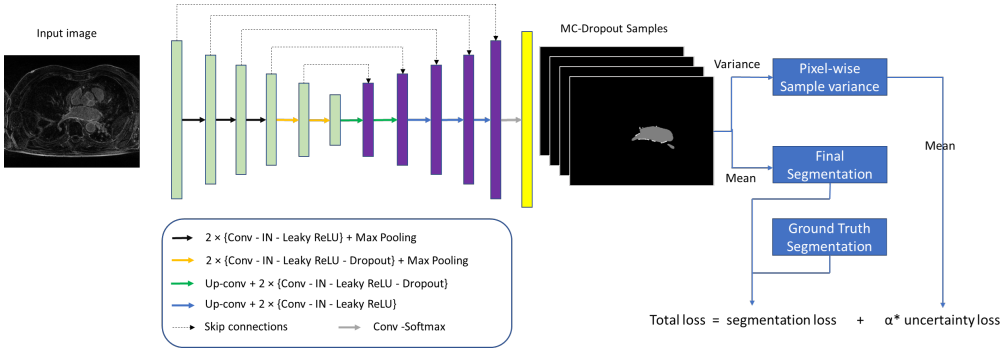

Fig. 1. Overview of the network architecture.

3.2 Loss functions

Recently, Leng et al. (2022) [13] proposed PolyLoss, a new loss function that expresses the commonly used loss functions such as cross-entropy (Eq. 1) and focal loss (Eq. 3) as a linear combination of polynomial functions. Using Taylor expansion, cross-entropy can be represented as sum of polynomial bases $(1-p)^j$, as shown in Eq. 2, where p is the prediction probability of the target class [13]. By dropping the higher-order polynomials and adding terms that perturb the polynomial coefficients, they came up with a simplified version of the polynomial loss called Poly-1. This loss function modifies the cross-entropy by only adding one hyper-parameter (ϵ) [13], as can be seen in Eq. 2. PolyLoss has shown good performance on computer vision tasks by outperforming cross-entropy and focal losses [13].

Inspired by [13], in this paper, we proposed a loss function that uses Dice loss with PolyLoss (Eq. 5) for a LA cavity and scar segmentation. Dice loss is a region based loss that directly optimizes the Dice coefficient metric as shown in Eq. 4. We hypothesized that by combining the region based Dice loss with the polynomial version of the cross-entropy (PolyCE) (Eq. 5) can improve the segmentation of LA cavity from multi-center LGE MRIs.

$$L_{CE} = -log(p) = \sum_{n=1}^{\infty} \frac{1}{n}(1-p)^n, \tag{1}$$

$$L_{PolyCE} = L_{CE} + \epsilon(1-p), \tag{2}$$

$$L_{Focal} = -(1-p)^{\gamma} log(p), \tag{3}$$

$$L_{Dice} = 1 - \frac{2|Y \cap G|}{|Y| + |G|}, \tag{4}$$

$$L_{DicePolyCE} = L_{Dice} + L_{PolyCE}, \tag{5}$$

where Y and G represent the predicted and manual segmentation maps, respectively.

Arega et al. (2021) [2] proposed a segmentation model that generates uncertainty estimates (sample variance) during training using the Monte-Carlo-dropout Bayesian method and utilizes the uncertainty information to enhance the segmentation results by incorporating it into the segmentation loss function [2]. During training, the model is sampled N times, and the mean of these samples is used as the final segmentation. The sample variance (uncertainty) (σ_i) is computed as a variance of the N Monte-Carlo prediction samples of each pixel i [2]. Since sample variance is a pixel-wise uncertainty measure, to determine the image-level uncertainty the mean of the pixel-wise uncertainty values is computed as shown in Eq. 7, where I is the total number of pixels of the image [2]. This image-level uncertainty is considered as uncertainty loss. Then, it is added to a segmentation loss with a hyper-parameter value alpha (α) that controls the contribution of the uncertainty loss to the total loss as shown in Eq. 8. They have shown that uncertainty information can be advantageous, particularly to improve the segmentation of semantically and visually challenging pathologies such as scars which generate higher epistemic uncertainty [2].

In this paper, we proposed to adopt the uncertainty loss in combination with the hybrid loss of Dice and Focal (DiceFocal) loss [33] (Eq. 6) for LA scar segmentation. We hypothesized that by fusing DiceFocal loss, which has shown good performance on highly imbalanced dataset [20], with the uncertainty loss (Uncertainty DiceFocal Loss) (Eq. 8) can enhance the segmentation of the more challenging LA scar segmentation.

$$L_{Seg(DiceFocal)} = L_{Dice} + L_{Focal}, \tag{6}$$

$$L_{Uncertainty} = \frac{1}{I}\sum_{i}(\sigma_i^2), \tag{7}$$

$$L_{Total(UncertaintyDiceFocalLoss)} = L_{Seg(DiceFocal)} + \alpha \times L_{Uncertainty}, \tag{8}$$

3.3 Data Augmentations

We applied a variety of data augmentations to improve the generalization and robustness of the models in the multi-center dataset, including intensity-based data augmentation, spatial data augmentation, and histogram matching augmentation [3, 9]. Histogram matching is the transformation of an image so that the histogram of a source image matches the histogram of a reference image [8]. Mathematically, it is the process of altering one image so that the cumulative distribution function (CDF) of values in each band corresponds to the CDF of bands in another image.

In the LAScarQS 2022 challenge, there was no specific information about each training image regarding the clinical center from which they came from. In this work, we used histogram matching by taking random training images and matching them to a selected low performing training images which had the

worst performance in terms of Dice. The matched images were then added to the training dataset to enhance the generalizability of the model on LA cavity segmentation from multi-Center LGE MRIs.

3.4 Training

The segmentation models were trained for 1000 epochs in a 5-fold cross-validation scheme. Stochastic gradient descent (SGD) with Nesterov momentum ($\mu = 0.99$) with an initial learning rate of 0.01 was used to optimize the network's weights. The learning rate was decayed using the "poly" learning rate policy [9]. We employed a mini-batch size of 2. We used a value of 1 for epsilon (ϵ) in PolyLoss (Eq. 2) and a value of 2 for gamma (γ) in Focal loss (Eq. 3). For the uncertainty loss, the weighting factor (α) (in Eq. 8) is empirically selected to be 2.0. For histogram matching, we utilized Simple ITK's python library [19]. The training was done on NVIDIA GPUs using Pytorch deep learning framework based on nnU-Net implementation [9].

4 Results and Discussion

To evaluate LA cavity segmentation, Dice coefficient, average surface distance (ASD) and Hausdorff distance (HD) metrics were used. For LA scar segmentation and quantification, accuracy, specificity, sensitivity, Dice coefficient of the scar, and generalized Dice score of the cavity and scar were used [16]. All the comparisons were done on the validation set provided by the challenge. The validation dataset for LA scar segmentation consists of 10 cases from center 1, the same center as the training dataset. For LA cavity segmentation which focuses on a multi-center problem, the validation dataset contains 10 cases from center 1, the same center as the training dataset, and 10 cases from center 2.

The baseline method is the standard nnU-Net network [9] with Dropout layers added at the middle layers of the segmentation network as mentioned in Section 3.1. It uses light data augmentation that includes rotation, scaling, Gaussian blur and noise. In terms of the loss function, the baseline method employs a hybrid loss of Dice loss with cross-entropy Loss (DiceCE).

Regarding the data augmentation, we separated the experiments into light data augmentation (baseline), moderate data augmentation and histogram matching augmentation. The same network architecture was used during the comparison. The moderate data augmentation uses elastic deformation, rotation, scaling, mirroring, additive brightness, Gaussian noise and blurring. For histogram matching (HM) augmentation, the matched images were added to the training dataset as mentioned in Section 3.3.

Comparing the data augmentation experiments' performance in Table 1, it can be observed that moderate data augmentation improved the segmentation performance from $17.1836mm$ to $16.8721mm$ in terms of HD. However, it yielded a bit worse result in both Dice and ASD compared to the baseline (light data

augmentation). Similarly, the histogram matching-based data augmentation significantly decreased the HD from 17.1836mm to 16.6851mm. However, its performance was slightly lower in terms of Dice score and ASD.

Comparing the performance of the loss functions on the segmentation of LA cavity, the proposed loss outperformed the other loss functions as shown in Table 1. The baseline (DiceCE loss) yielded a Dice score of 0.8884, ASD of 1.74629 and HD of 17.18363 mm whereas DiceFocal loss achieved a Dice score of 0.8885, ASD of 1.7474 and HD of 17.2035 mm. Using only the polynomial version of cross-entropy loss (PolyCE) enhanced the segmentation result mainly in terms of Dice score and HD. When PolyCE is combined with Dice loss, the segmentation result of LA cavity was improved further from 0.8884 to 0.8897, from 1.7463 to 1.7203, and from 17.1836 to 16.9067 mm in terms of Dice score, ASD and HD respectively compared to the baseline which uses DiceCE loss.

Table 2 shows the comparison of the different loss functions on LA scar segmentation. Compared to LA cavity segmentation, it has imbalanced classes because the scar is very small compared to the cavity. Due to this, we have compared the proposed loss not only to the baseline but also to other loss functions which are commonly used for imbalanced segmentation. For example, hybrid loss functions such as DiceFocal loss [33], and DiceTopK loss [4] which combines Dice loss with Focal loss and TopK loss respectively to mitigate class imbalance [20]. In the comparison, we have also included Focal loss [18], a loss function that was designed to deal with foreground-background class imbalance by focusing more on the hard examples.

Table 1. Comparison of LA cavity segmentation performance using various data augmentations and compound loss functions on validation set ($n = 20$) of the challenge. Dice: Dice score, ASD: average surface distance, HD: Hausdorff distance. The bold values are the best.

Method	**Dice**	**ASD**	**HD (mm)**
Baseline	0.8884	1.7463	17.1836
Moderate DataAug	0.8868	1.7755	16.8721
HM DataAug	0.8867	1.7536	**16.6851**
DiceFocal	0.8885	1.7474	17.2035
OnlyPolyCE	0.8893	1.7413	17.0053
Proposed (DicePolyCE)	**0.8897**	**1.7203**	16.9067

As shown in Table 2, the baseline, which combines Dice loss with cross-entropy loss (DiceCE) [9], yielded an accuracy of 0.7764, sensitivity of 0.5529, Dice score of 0.6258 and generalized Dice score 0.9187 for scar segmentation. The DicePolyCE loss enhanced the performance of baseline as it increased the accuracy, sensitivity, Dice and generalized Dice of scar by 22%, 1%, 0.5%, 0.01%, respectively. DiceTopK loss [4] achieved an accuracy of 0.7751, sensitivity of 0.5503, Dice score of 0.6222 and generalized Dice score 0.9183 which is lower than the baseline. Using only Focal loss [18] achieved the worst result as can

be seen in Table 2. The other commonly used loss function for an imbalanced dataset that is DiceFocal loss [33] yielded much better result compared to the baseline, DicePolyCE and DiceTopK loss with an accuracy of 0.9999, sensitivity of 0.5749, Dice score of 0.6363 and generalized Dice score 0.9199. The proposed loss, where uncertainty loss is combined with DiceFocal loss achieved the best result outperforming the other loss functions. In terms of specificity, all the loss functions achieved a similar score of 0.9999.

From the results, we observed that a compound loss that utilizes Dice loss with the polynomial version of cross-entropy loss (DicePolyCE) consistently improves the performance of the most common compound loss that combines Dice loss with cross-entropy loss. The performance enhancement was in both the mildly imbalanced LA cavity segmentation and the highly imbalanced LA scar segmentation. This shows the robustness of the proposed loss in LA cavity and scar segmentation.

In LA scar segmentation, the second proposed loss function which utilizes uncertainty information outperformed the commonly used loss functions for highly imbalanced segmentation such as DiceTopK [4] and Focal loss [18] functions [20], DiceFocal loss [33]. This confirms the importance of incorporating uncertainty information as part of the learning process to enhance particularly the segmentation of pathologies with irregular structures like scars.

Table 2. Comparison of LA scar segmentation performance using different compound loss functions on validation set ($n = 10$) of the challenge. GDice: generalized Dice score of cavity and scar. The bold values are the best.

Method	**Accuracy**	**Specificity**	**Sensitivity**	**Dice**	**GDice**
Baseline	0.7764	0.9999	0.5529	0.6258	0.9187
DiceTopK Loss	0.7751	0.9999	0.5503	0.6222	0.9183
DiceFocal Loss	0.9999	0.9999	0.5749	0.6363	0.9199
Focal Loss	0.9999	0.9999	0.5095	0.6047	0.9139
DicePolyCE Loss	0.9999	0.9999	0.5605	0.6301	0.9187
Proposed (Uncertainty+ DiceFocal Loss)	**0.9999**	**0.9999**	**0.5853**	**0.6406**	**0.9205**

In terms of data augmentation, the experiments were mainly focused on the multi-center LA cavity segmentation. From the results, we can say that using moderate data augmentation and histogram matching can enhance the model's generalization as it improved the segmentation result, particularly in terms of HD compared to the light data augmentation.

5 Conclusion

In this paper, we proposed a fully automatic deep learning method that utilizes a novel hybrid loss function that combines Dice loss with a polynomial

version of cross-entropy loss to segment LA cavity from multi-center LGE MRIs and an uncertainty-based loss function to segment scar from single-center LGE MRIs. We also employed various data augmentation techniques, which include histogram matching, to increase the size and variety of the training dataset. In the experiments, we have compared the proposed loss function with the commonly used losses in the multi-center LA cavity segmentation and in the highly imbalanced LA scar segmentation. We observe that the proposed losses yield the best result outperforming the other losses in both LA cavity and scar segmentation. From the results, we can say that using the polynomial version of cross-entropy in combination with Dice loss can be a better alternative loss function for anatomical segmentation such as LA cavity. For segmentation such as LA scar, which generates high epistemic uncertainty due to its small and complex structure, utilizing a loss function that incorporates uncertainty information can be useful for robust segmentation. Additionally, applying moderate-level data augmentation with histogram matching can improve the results and increase the model's generalization capability.

6 Acknowledgements

This work was supported by the French National Research Agency (ANR), with reference ANR-19-CE45-0001-01-ACCECIT. Calculations were performed using HPC resources from DNUM CCUB (Centre de Calcul de l'Université de Bourgogne) and from GENCI–IDRIS (Grant 2022-AD011013506). We also thank the Mesocentre of Franche-Comté for the computing facilities.

References

1. Arega, T.W., Bricq, S.: Automatic myocardial scar segmentation from multi-sequence cardiac mri using fully convolutional densenet with inception and squeeze-excitation module. In: Myocardial Pathology Segmentation Combining Multi-Sequence CMR Challenge. pp. 102–117. Springer (2020)
2. Arega, T.W., Bricq, S., Meriaudeau, F.: Leveraging uncertainty estimates to improve segmentation performance in cardiac mr. In: Uncertainty for Safe Utilization of Machine Learning in Medical Imaging, and Perinatal Imaging, Placental and Preterm Image Analysis, pp. 24–33. Springer (2021)
3. Arega, T.W., Legrand, F., Bricq, S., Meriaudeau, F.: Using mri-specific data augmentation to enhance the segmentation of right ventricle in multi-disease, multi-center and multi-view cardiac mri. In: International Workshop on Statistical Atlases and Computational Models of the Heart. pp. 250–258. Springer (2021)
4. Brugnara, G., Isensee, F., Neuberger, U., Bonekamp, D., Petersen, J., Diem, R., Wildemann, B., Heiland, S., Wick, W., Bendszus, M., et al.: Automated volumetric assessment with artificial neural networks might enable a more accurate assessment of disease burden in patients with multiple sclerosis. European Radiology **30**(4), 2356–2364 (2020)
5. Chen, C., Bai, W., Rueckert, D.: Multi-task learning for left atrial segmentation on ge-mri. In: STACOM@MICCAI (2018)

6. Clinic, M.: Atrial fibrillation - symptoms and causes (2021), https://www.mayoclinic.org/diseases-conditions/atrial-fibrillation/symptoms-causes/syc-20350624
7. Gao, Y., Gholami, B., Macleod, R., Blauer, J.J.E., Haddad, W.M., Tannenbaum, A.R.: Segmentation of the endocardial wall of the left atrium using local region-based active contours and statistical shape learning. In: Medical Imaging (2010)
8. Gorelick, N.: Histogram matching (2021), https://medium.com/google-earth/histogram-matching-c7153c85066d
9. Isensee, F., Jaeger, P., Kohl, S., Petersen, J., Maier-Hein, K.: nnU-Net: a self-configuring method for deep learning-based biomedical image segmentation. Nature Methods **18**, 1–9 (02 2021). https://doi.org/10.1038/s41592-020-01008-z
10. Jamart, K., Xiong, Z., Talou, G.D.M., Stiles, M.K., Zhao, J.: Two-stage 2d cnn for automatic atrial segmentation from lge-mris. In: STACOM@MICCAI (2019)
11. Karim, R., Arujuna, A., Housden, R.J., Gill, J., Cliffe, H., Matharu, K., Gill, J.S., Rindaldi, C.A., O'Neill, M.D., Rueckert, D., Razavi, R., Schaeffter, T., Rhode, K.S.: A method to standardize quantification of left atrial scar from delayed-enhancement mr images. IEEE Journal of Translational Engineering in Health and Medicine **2**, 1–15 (2014)
12. Karim, R., Housden, R.J., Balasubramaniam, M., Chen, Z., Perry, D., Uddin, A., Al-Beyatti, Y., Palkhi, E., Acheampong, P., Obom, S., Hennemuth, A., Lu, Y., Bai, W., Shi, W., Gao, Y., Peitgen, H.O., Radau, P.E., Razavi, R., Tannenbaum, A.R., Rueckert, D., Cates, J.E., Schaeffter, T., Peters, D.C., Macleod, R., Rhode, K.S.: Evaluation of current algorithms for segmentation of scar tissue from late gadolinium enhancement cardiovascular magnetic resonance of the left atrium: an open-access grand challenge. Journal of Cardiovascular Magnetic Resonance **15**, 105 – 105 (2013)
13. Leng, Z., Tan, M., Liu, C., Cubuk, E.D., Shi, X., Cheng, S., Anguelov, D.: Polyloss: A polynomial expansion perspective of classification loss functions. ArXiv **abs/2204.12511** (2022)
14. Li, L., Wu, F., Yang, G., Xu, L., Wong, T., Mohiaddin, R., Firmin, D., Keegan, J., Zhuang, X.: Atrial scar quantification via multi-scale cnn in the graph-cuts framework. Medical image analysis **60**, 101595 (2020)
15. Li, L., Zimmer, V.A.M., Schnabel, J.A., Zhuang, X.: Atrialgeneral: Domain generalization for left atrial segmentation of multi-center lge mris. In: MICCAI (2021)
16. Li, L., Zimmer, V.A.M., Schnabel, J.A., Zhuang, X.: Atrialjsqnet: A new framework for joint segmentation and quantification of left atrium and scars incorporating spatial and shape information. Medical image analysis **76**, 102303 (2022)
17. Li, L., Zimmer, V.A.M., Schnabel, J.A., Zhuang, X.: Medical image analysis on left atrial lge mri for atrial fibrillation studies: A review. Medical image analysis **77**, 102360 (2022)
18. Lin, T.Y., Goyal, P., Girshick, R., He, K., Dollár, P.: Focal loss for dense object detection. In: Proceedings of the IEEE international conference on computer vision. pp. 2980–2988 (2017)
19. Lowekamp, B.C., Chen, D.T., Ibáñez, L., Blezek, D.J.: The design of simpleitk. Frontiers in Neuroinformatics **7** (2013)
20. Ma, J., Chen, J., Ng, M., Huang, R., Li, Y., Li, C., Yang, X., Martel, A.L.: Loss odyssey in medical image segmentation. Medical image analysis **71**, 102035 (2021)
21. Moccia, S., Banali, R., Martini, C., Muscogiuri, G., Pontone, G., Pepi, M., Caiani, E.G.: Development and testing of a deep learning-based strategy for scar segmentation on cmr-lge images. Magnetic Resonance Materials in Physics, Biology and Medicine **32**, 187–195 (2018)

22. Oakes, R.S., Badger, T.J., Kholmovski, E.G., Akoum, N., Nathan, S.S., Burgon, Fish, E.N., Blauer, J.J.E., Rao, S.N., DiBella, E.V.R., Nathan, M., Segerson, Daccarett, M., Windfelder, J., McGann, C., Dennis, Parker, Macleod, R., Marrouche, N.F.: Detection and quantification of left atrial structural remodeling using delayed enhancement mri in patients with atrial fibrillation (2009)
23. Perry, D., Morris, A.K., Burgon, N., McGann, C., Macleod, R., Cates, J.E.: Automatic classification of scar tissue in late gadolinium enhancement cardiac mri for the assessment of left-atrial wall injury after radiofrequency ablation. In: Medical Imaging (2012)
24. Ravanelli, D., dal Piaz, E.C., Centonze, M., Casagranda, G., Marini, M., Greco, M.D., Karim, R., Rhode, K.S., Valentini, A.: A novel skeleton based quantification and 3-d volumetric visualization of left atrium fibrosis using late gadolinium enhancement magnetic resonance imaging. IEEE Transactions on Medical Imaging **33**, 566–576 (2014)
25. Tao, Q., Ipek, E.G., Shahzad, R.K., Berendsen, F.F., Nazarian, S., van der Geest, R.J.: Fully automatic segmentation of left atrium and pulmonary veins in late gadolinium-enhanced mri: Towards objective atrial scar assessment. Journal of Magnetic Resonance Imaging **44** (2016)
26. Vesal, S., Ravikumar, N., Maier, A.K.: Dilated convolutions in neural networks for left atrial segmentation in 3d gadolinium enhanced-mri. ArXiv **abs/1808.01673** (2018)
27. Wilber, D.J., Pappone, C., Neuil, P., de Paola, Â.A.V., Marchlinski, F.E., Natale, A., Macle, L., Daoud, E.G., Calkins, H., Hall, B., Reddy, V., Augello, G., Reynolds, M.R., Vinekar, C., Liu, C.Y., Berry, S.M., Berry, D.A.: Comparison of antiarrhythmic drug therapy and radiofrequency catheter ablation in patients with paroxysmal atrial fibrillation: a randomized controlled trial. JAMA **303 4**, 333–40 (2010)
28. Xia, Q., Yao, Y., Hu, Z., Hao, A.: Automatic 3d atrial segmentation from ge-mris using volumetric fully convolutional networks. In: STACOM@MICCAI (2018)
29. Yang, G., Chen, J., Gao, Z., Li, S., Ni, H., Angelini, E.D., Wong, T., Mohiaddin, R.H., Nyktari, E., Wage, R., Xu, L., Zhang, Y., Du, X., Zhang, H., Firmin, D.N., Keegan, J.: Simultaneous left atrium anatomy and scar segmentations via deep learning in multiview information with attention. Future Generations Computer Systems **107**, 215 – 228 (2020)
30. Yang, X., Wang, N., Wang, Y., Wang, X., Nezafat, R.V., Ni, D., Heng, P.A.: Combating uncertainty with novel losses for automatic left atrium segmentation. ArXiv **abs/1812.05807** (2018)
31. Zabihollahy, F., White, J.A., Ukwatta, E.: Myocardial scar segmentation from magnetic resonance images using convolutional neural network. In: Medical Imaging (2018)
32. Zhu, L., Gao, Y., Yezzi, A.J., Tannenbaum, A.R.: Automatic segmentation of the left atrium from mr images via variational region growing with a moments-based shape prior. IEEE Transactions on Image Processing **22**, 5111–5122 (2013)
33. Zhu, W., Huang, Y., Zeng, L., Chen, X., Liu, Y., Qian, Z., Du, N., Fan, W., Xie, X.: Anatomynet: Deep learning for fast and fully automated whole-volume segmentation of head and neck anatomy. Medical Physics **46**, 576–589 (2019)